Article

# EEG characterization and classification based on image gradient histograms

**Rodrigo Ramele [1,†*], Ana Julia Villar [1] and Juan Miguel Santos [1]**

[1] Computer Engineering Department, Instituto Tecnológico de Buenos Aires (ITBA); info@itba.edu.ar
* Correspondence: rramele@itba.edu.ar; Tel.: +54-9-11-4193-9382
† Current address: C1437FBH Lavarden 315, Ciudad Autónoma de Buenos Aires, Argentina

Academic Editor: name
Version September 15, 2017 submitted Typeset by LaTeX

**Abstract:** The analysis of Electroencephalography (EEG) signals is of ulterior importance to elucidate patterns that could improve the implementation of Brain Computer Interfaces (BCI). These systems are meant to provide alternative pathways to transmit volitional information which could potentially enhance the quality of life of patients affected by neurodegenerative disorders or improve Human Computer Interaction systems. Of particular interests are those which are based on the recognition of Event-Related Potentials (ERP) because they can be elicited by external stimuli and used to implement spellers, to control external devices or even avatars in virtual reality environments. This work mimics what electroencephalographers have been doing clinically, visually inspecting and categorizing phenomena within the EEG by the extraction of features from the images of the plots of the signals. It also aims to provide a framework to analyze, characterize and classify EEG signals, with a focus on the P300, an ERP elicited by the oddball paradigm of rare events. The validity of the method is shown by offline processing a public dataset of Amyotrophic Lateral Sclerosis (ALS) patients.

**Keywords:** electroencephalography (EEG); BCI; P300; ALS; classification; HOG; SIFT

---

## 0. Introduction

Although recent advances in neuroimagining techniques (particularly radio-nuclear and radiological scanning methods) [1] have diminished the prospects of the traditional Electroencephalography (EEG), the advent and development of digitalized devices has pressed for a revamping of this hundredth years old technology. Their versatility, ease of use, temporal resolution, ease of development and fabrication, and its proliferation as consumer devices, are pushing EEG to become the de-facto non invasive portable or ambulatory method to access and harness brain information [2]

A key contribution to this expansion has been the field of Brain Computer Interfaces (BCI) [3] which is the pursuit of the development of a new channel of communication particularly aimed to persons affected by neuro-degenerative diseases.

One noteworthy aspect of this novel communication channel is the ability to volitionally transmit information from the Central Nervous System (CNS) to a computer device and from there use that information to control a wheelchair [4], as input to a speller application [5], in a Virtual Reality environment [6] or as aiding tool in a rehabilitation procedure [7]. The holly grail of BCI is to implement a new complete and alternative pathway to restore lost locomotion [3].

EEG signals are remarkably complex and have been characterized as a multichannel non-stationary stochastic process. Additionally, they have high variability between different subjects and even between different moments for the same subject, requiring adaptive and co-adaptive calibration and learning procedures [8]. Hence, this imposes an outstanding challenge that is necessary to overcome in order to extract information from raw EEG signals.

Moreover, EEG markers [8] that can be used to volitionally transmit information are limited, and each one of them has a particular combination of appropriate methods to decode them. Inevitably, it is necessary to implement many distinct and specialized algorithmic methods, to filter the signal, enhance its SNR, and try to determine some meaning out of it.

BCI has gained mainstream public awareness with worldwide challenge competitions like Cybathlon [9] and even been broadcasted during the inauguration ceremony of the 2014 Soccer World Cup. New developments have overcome the out-of-the-lab high-bar and they are starting to be used in real world environments [10]. However, they still lack the necessary robustness, and its performance is well behind any other method of human computer interaction, including any kind of detection of residual muscular movement [8].

In this work, a new method to characterize and classify EEG signals is presented, expanded and detailed. Its validity is verified by processing offline data for ALS patients. This is the continuation of the work previously presented in [11], where it was applied to rhythmic patterns, and that it can be extended to describe transient events like those produced by P300 Event Related Potential [12].

The method is based on the morphological analysis of the shape of the EEG signal [13,14] and was inspired by mimicking what traditionally electroencephalographers have been performing for almost a century: visually inspecting raw signal plots [15].

This paper reports a straightforward method to, (1) characterize EEG signals based on the identification of their structure in the shape domain using the histogram of gradients extracted from the signal plot, and (2) how this characterization can be used to implement a BCI classification scheme to identify Event Related Potentials, particularly the well-known P300, on an offline and public dataset.

This article unfolds as follows: in Section 1 the Feature Extraction based on Histogram of Gradients of the Signal Plot method is explained: section 1.b describes how the image of the signal plot is constructed whereas section II describes in detail the feature extraction procedure. Section III.b presents the classification algorithm based on NBNN classification and in the final section shows a discussion and we expose our remarks, conclusions and future work.

## 1. Materials and Methods

### *1.1. Feature Extraction based on Histogram of Gradients of the Signal Plot*

The P300 [12] is a positive deflection of the EEG signal which occurs 300 ms after the onset of a rare and deviant stimulus that the subject is expected to attend. It is produced under the oddball paradigm [3] and though it is quite consistent across different subjects, it has a lower amplitude ( $\pm 5 \mu V$ ) compared to basal EEG activity reaching a SNR [illegible] around -15 db estimated based on the amplitude of the P300 response signal divided by the S[illegible] the background EEG activity [16]. This signal can be used to implement a speller application by using a Speller Matrix [17] (Fig. 1) where the flashings of rows and columns provide the deviant stimulus required to elicit this physiological response. Each time a row or column that contain the desired letter flashes, the corresponding synchronized EEG signal should also contain the P300 signature and by detecting it, the selected letter can be identified.

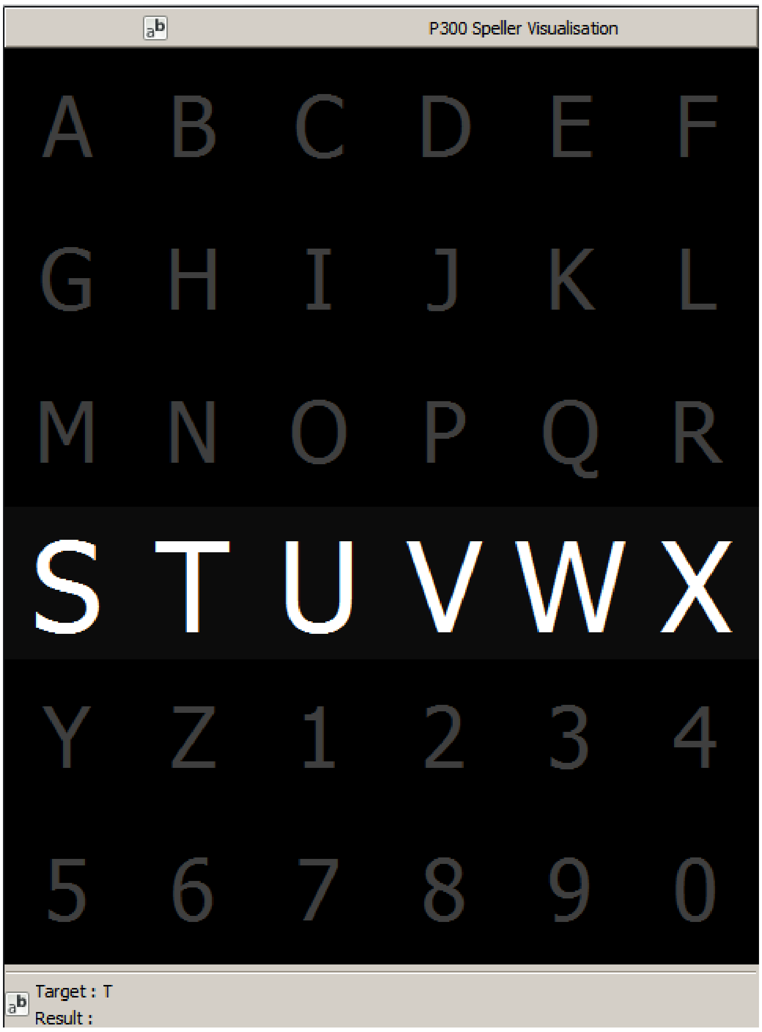


**Figure 1.** The P300 Matrix[17] used in the OpenVibe Open Source software [18]. Rows are labeled from 1 to 6 and columns from 7 to 12. Rows/columns flash intermittently in a random order.

### 1.1.1. Preprocessing

The first step consists of the enhancement of the SNR of the P300 pattern above the level of basal EEG. The processing pipeline starts by applying a notch filter to the raw signal, a 4th degree 10 Hz lowpass Butterworth filter and finally a decimation with an FIR filter of order 30 from the original 250 Hz down to 16 Hz.

### 1.1.2. Artefact Removal, Segmentation and Signal Averaging

- **Artefact Removal**: The EEG signal matrix is processed on a channel by channel basis. For every 12 flashing stimuli, i.e. one complete sequence of intensification of each of the 6 rows plus the 6 columns, a basic artefact elimination procedure is implemented by removing the entire segment when any signal deviates above/bellow $\pm 70 \mu V$.
- **Segmentation**: For each of the 12 stimuli, a window of 1 second of the multichannel signal is extracted, starting from the stimulus onset, corresponding to each row/column intensification. Two of these segments are labeled as *hit*, whereas the remaining 10 are labeled as *no hit*. A hit represents that the EEG segment should contain the ERP signature time-locked to the flashing stimulus.
- **Signal Averaging**: The P300 ERP is deeply buried under background EEG so the traditional approach to identify it is by point-to-point averaging the time-locked stacked signal segments.

Hence the values which are not related to, and not time-locked to the onset of the stimulus are canceled out (they have zero mean) [19].

This last step determines the operation of any P300 Speller. In order to obtain an improved signal in terms of its SNR, repetitions of the sequence of row/column intensification is necessary. And, at the same time, as long as more repetitions are needed, the ability to transfer information faster is diminished, so there is a trade-off that must be acutely determined.

#### 1.1.3. Signal Plotting

The underlying idea of this method is to generate a template for the signal, based on the image plot. Hence, the first step is its transformation into a temporary binary image.

The signal is first scaled and normalized (i.e. z-score) by

$$\tilde{x}(t,c) = \left\lfloor \gamma \cdot \frac{(x(t,c) - \bar{x}(t,c))}{\sigma_x(c)} \right\rfloor \tag{1}$$

where $\gamma$ is the image scale, $t$ is the time and $x(t,c)$ is the point-to-point averaged EEG matrix defined for each $t$ and for a channel $c$, and $\bar{x}(t,c)$ and $\sigma_x$ are the mean and standard deviation of $x$.

Then the image is constructed by locating the available sample points according to

$$I(z_1, z_2) = \begin{cases} 255 & z_1 = \gamma \cdot t; z_2 = \tilde{x}(t,c) + z(c) \\ 0 & \text{otherwise} \end{cases} \tag{2}$$

In order to construct the plot from the pixels, the Bresenham [11] algorithm is used to interpolate a straight line between each pair of these consecutive pixels.

#### 1.1.4. Feature Extraction: Histogram of Oriented Gradients

On the generated image, a keypoint is placed on a precise location along the signal trace over the image plot. Around that center, a local image patch is constructed as follows: it is first divided in 16 blocks, arranged in a 4x4 grid and centered on $T = (x,y)$.

A local representation of the shape of the signal within the patch can be described by obtaining the gradient orientations on each of the 16 blocks and creating a histogram of the oriented gradients. This technique is based on Lowe's SIFT [20] descriptor, and it is biomimetically inspired in how the visual cortex detects shapes by analyzing orientations. In order to calculate this histogram, the interval $[0-360]$ of possible angles is divided in 8 bins, each one at 45 degrees (Fig 2).

The values of the image gradients for the 8 angle bins $p = 0, 45, 90, 135, 180, 225, 270$ and for each grid block bin $i, j = 1, 2, 3, 4$ are accumulated in the 3-dimensional histogram $h$ through

$$h(p,i,j) = 3 \cdot s \int w_{\text{ang}}(\angle J(\mathbf{x}) - \theta_p)\, w_{ij} \left( \frac{\mathbf{x} - T}{3s} \right) |J(\mathbf{x})|\, d\mathbf{x} \tag{3}$$

where $s$ is the size of the local patch, which can be converted into pixels by doing $Px = 4 \cdot 3 \cdot s$ , $|J(\mathbf{x})|$ is the norm of the gradient vector found at each one of the 16 blocks of the patch, whereas $\angle J(\mathbf{x})$ is the angle of the gradient vector and $\theta_p$ is one of the bin angles. On the other hand $x = (x_i, x_j)$ corresponds to each one of the pixels of the local patch, and $w_{\text{ang}}$ and $w_{ij}$ are linear interpolation functions [20]. Finally, the magic value of 3 is a magnification factor which corresponds to the number of pixels for each grid block when the size of the patch is the unity.

Finally, as the patch is 4x4, it gives a descriptor of 128 dimension as shown on Figure 2.

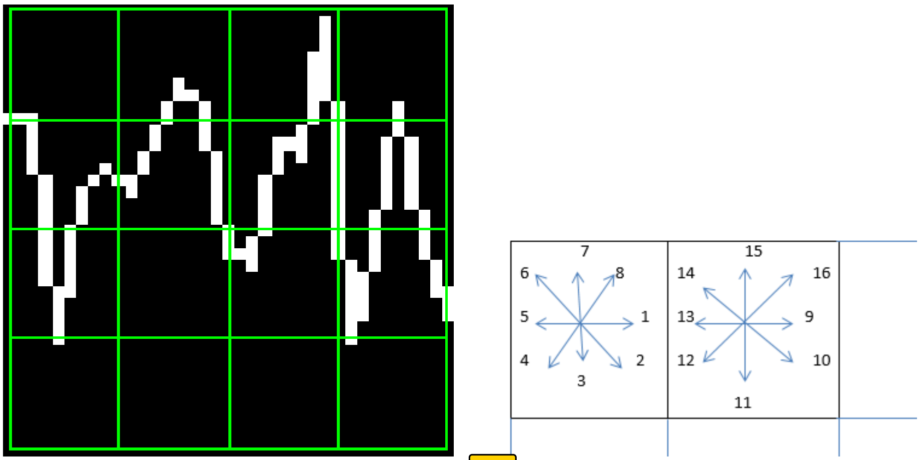


**Figure 2.** (Left) The local patch is located on a precise location within the generated plot. The 4x4 block grid can be seen on the patch. (Right) On each grid block, eight bins are used to describe the eight different orientations, so the first block picks the first eight orientations.

#### 1.1.5. Classification

The classification is carried out by using a discriminative semi-supervised classification method, the Naive Bayes Nearest Neighbout (NBNN) [22] and the first step consists in extracting labelled descriptors from the training set for each class, which are thus grouped together in two KD-tree [21] database structures.

While doing classification based on local features, which encode partial information, one problem that frequently arises is how to ensemble the individual classification of each local characteristic to the image that were used to derive those descriptors.

The NBNN algorithm tackles this problem by comparing each image against a whole classification class which is characterized by the set of descriptors that are closest to each one of the descriptors obtained for the query image. The algorithm is based on 4,

$$\hat{C} = argmin_C \sum \|d_i - NN_C(d_i)\|^2 \tag{4}$$

where the predicted class $\hat{C}$ of a query image is calculated as the class $C$ that minimize the summation of the $L^2$ distance between each descriptor $d_i$ that belongs to the query image and its corresponding near neighbour $NN_C(d_i)$ descriptor from each class.

### *1.2. Experimental Protocol*

To verify the validity of the proposed framework and method, the public dataset 008-2014 [23] published on the BNCI-Horizon website [24] by IRCCS Fondazione Santa Lucia, was used to perform an offline BCI Simulation to decode the spelled words from the provided signals. The algorithm was implemented using VLFeat [21] Computer Vision libraries on MATLAB 2014a (Mathworks Inc., Natick, MA, USA).

#### 1.2.1. P300 ALS Public Dataset

The experimental protocol used to generate this dataset is explained in [23] but can be summarized as follows: 8 subjects with confirmed diagnoses but on different stages of ALS disease, were recruited and accepted to perform the experiments. The P300 detection task designed for this experiment consisted of spelling 7 words (runs) of 5 letters each, using the traditional P300 Speller Matrix [17] where the flashings of rows and columns provide the deviant stimulus required to elicit this physiological response. The first 3 runs were used for training and the remaining 4 for testing with visual feedback. A trial, as defined by the BCI2000 platform [25], was every attempt to select a letter from the speller, and it was composed of signal segments corresponding to 10 repetitions of flashes of 6 rows and 6 columns of the traditional 6x6 P300 matrix , yielding 120 repetitions. Flashing of row/columns was performed for 0.125 s, following by a resting period (i.e. Inter-stimulus interval) of the same length. After 120 repetitions an inter-trial pause was included before resuming with the following letter.

The recorded dataset was sampled at 256 Hz and consisted of an EEG matrix for electrode channels Fz,Cz,Pz,Oz,P3,P4,PO7 and PO8, identified according to the 10-20 International System, for each one of the 8 subjects.

In order to asses and verify the identification of the P300 response, subjects are instructed to a copy-spelling task where they have to fix their attention to successive letters in order to copy a previously determined set of words (in contrast to an online free-running operation of the speller where each users decides on its own what to spell).

### 1.2.2. Parameters

This method's parameters were selected according to the experimental protocol. As the P300 event latency and amplitude variate greatly between subjects, it is necessary to provide a descriptor that will be able to capture an entire transient event. Equations 5 and 6 can be used to map the original signal parameters to local image patch structure.

$$s = \frac{\Delta \mu V}{4 \cdot 3} \cdot \gamma \tag{5}$$

$$s = \frac{\lambda \cdot Fs}{4 \cdot 3} \cdot \gamma \tag{6}$$

where $Fs$ is the sample frequency of the EEG signal, $\lambda$ is the length in seconds covered by the patch, and $\mu V$ corresponds to the amplitude in microvolts that can be covered by the height of the patch. By using $s = 3$ and a quadruple scale of the image $\gamma = 4$ this gives the local patch, and the descriptor, the ability to identify events of 18 $\mu V$ of amplitude of $\lambda = 0.5s$. Finally, descriptors locations $T$ were selected as suggested by the dataset publisher [23] between 0.2s and 0.7s after the onset of the stimulus.

## 2. Results

In Figure 3 the grand average (point-to-point) for all the subjects using the whole trial (i.e. 120 repetitions) is shown. The P300 characteristic curve can be seen particularly in subjects 2, and 6 and in a lesser extend in the remaining subjects. In order to obtain a valid binary classification on averaged signals, particular care was observed to avoid unbalanced samples, because that may introduce a bias in the classification procedure (the variance of average signals is inversely proportional to the number of samples and the procedure would be discriminating signals with different variances). Especially in the case of the P300 response, the oddball paradigm requires that one of the stimuli need to be infrequent so that will unavoidably force the data to be unbalanced (i.e. an unequal number of trials in each condition) [26].

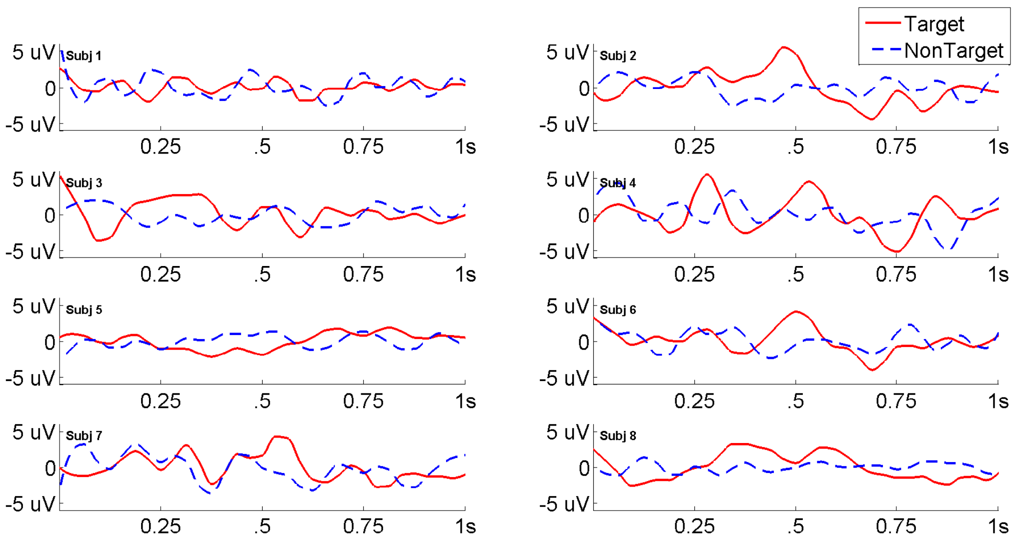


**Figure 3.** Point-To-Point grand averages of epochs obtained for hits (solid line) and no hits (dashed line) for each one of the 8 subjects for channel Cz. The P300 characteristic curve can be well identified particularly on subjects 2 and 6.

Results are shown in Table 1 where percentage of correctly spelled letters from the Cz channel is calculated while performing an offline BCI Simulation. Additionally the best performing channel is informed as well as its percentage of correct letters. It is of particular interest that using this method, the best performing channel was not always Cz, and instead occipital channels PO8 and PO7 showed very good performance indeed [7,10].

**Table 1.** Percentage of correctly predicted letters while performing an offline BCI Simulation for the best performing channel for each subject. Chance level is 0.02

| Participant | BPC | Performance |
|---|---|---|
| 1 | Cz | 0.35 |
| 2 | Fz | 0.85 |
| 3 | Cz | 0.25 |
| 4 | PO8 | 0.55 |
| 5 | PO7 | 0.40 |
| 6 | PO7 | 0.60 |
| 7 | PO8 | 0.80 |
| 8 | PO7 | 0.95 |

The ITR or BTR, in the case of reactive BCIs [3] strongly depends on the amount of signal averaging required to transmit a valid and robust selection. There is a trade-off that needs to be balanced between the required number of repetitions for each trial to guarantee robust transmission and the the achieved speed of transmission affected by the repetitions. As detailed in the table ... by applying this method, accuracy levels are only reduced in 20 percent even by using only one sequence of 12 repetitions (i.e. an entire flashing of the whole matrix).

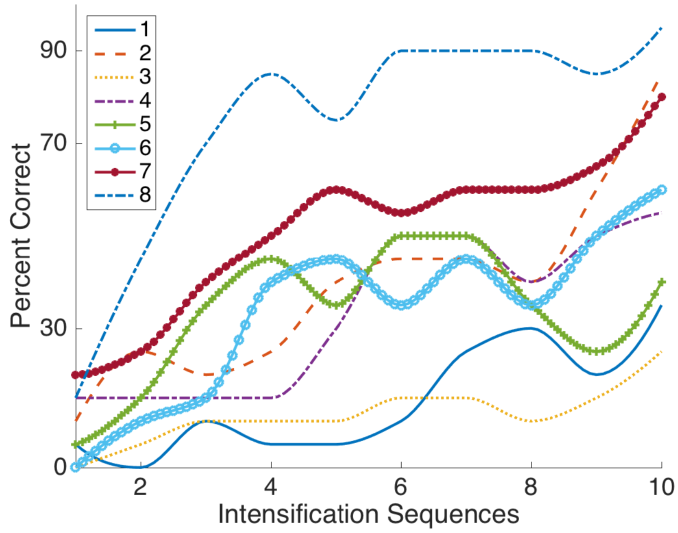


**Figure 4.** Point-To-Point graph averages of epochs obtained for hits (solid line) and no hits (dashed line) for each one of the 8 subjects for channel Cz. The P300 characteristic curve can be well identified particularly on subjects 2 and 6.

## 3. Discussion

This method, different from other methods which is based on the nonlinearity of the gradient of histograms which can be used to detect

is also based on how the image look like.

SNR of p300 and how to detect it

Check if you can use this to detect any kind of transient signal.

Compare if it is possible with the descriptors from one subject, discriminate the others.

Channal identification based on the metric distance between the bags

Signal Averaging.

## 4. Conclusion

A method to characterize and classify EEG signals where the main characteristic can be both, rhythmic in nature as in motor imagery, and also transient in time space, like the P300 has been presented.

Although single trial classification was not perfectly achieved, it has been shown that this method could be applied with a P300 Speller Matrix application with increased ITR.

The adaptive behaviour of the algorithm make it well suited when the shape of the pattern elicited by the P300 response, does not conform to the predicted structure. This is due to the fact that the descriptors are directly based on how the signals actually looked like for the training and calibration step, and they do not require any prior knowledge about the signal. This is of particular relevance for studies on outliers populations as may be the case for people who suffered some form of neuro-degenerative disorder like Lou Gehrig's disease.

The expanding of the understanding of this tool in order to automatically classify patterns in EEG, that are specifically identified by their shapes, is a prospect future work to be considered. It may also provide assistance to physician or electroencephalographers to help them locate these EEG patterns particularly in long recording periods [15], frequent in sleep research.

Moreover, this method can be used as an alternate *BCI predictor* [8] or as a tool for artefact removal (which is performed on many occasions by visually inspecting the signal).

**Acknowledgments:** This project was supported by the ITBACyT-15 funding program issued by ITBA University.

**Conflicts of Interest:** The authors declare no conflict of interest.

## Abbreviations

The following abbreviations are used in this manuscript:

EEG: electroencephalography
BCI: Brain Computer Interfaces
SNR: Signal to Noise Ratio
CNS: Central Nervous System
ALS: Amyotrophic Lateral Sclerosis
ERP: Event-Related Potential
P300: Positive deflection of an Event-Related Potential which occurs 300 ms after onset of stimulus
ITR: Information Transfer Rate
BTR: Bit Transfer Rate
SIFT: Scale Invariant Feature Transform
HOG: Histogram Of Gradients

## Bibliography

1. Schomer, D.L.; Silva, F.L.D. *Niedermeyer's Electroencephalography: Basic Principles, Clinical Applications, and Related Fields*; Vol. 1, 2010; p. 1296.
2. De Vos, M.; Debener, S. Mobile EEG: Towards brain activity monitoring during natural action and cognition. *International Journal of Psychophysiology* **2014**, *91*, 1–2.
3. Wolpaw, Jonathan R, W.E. *Brain-Computer Interfaces: Principles and Practice*; Oxford University Press, 2012; p. 400.
4. Carlson, T.; del R. Millan, J. Brain-Controlled Wheelchairs: A Robotic Architecture. *IEEE Robotics & Automation Magazine* **2013**, *20*, 65–73.
5. Guger, C.; Daban, S.; Sellers, E.; Holzner, C.; Krausz, G.; Carabalona, R.; Gramatica, F.; Edlinger, G. How many people are able to control a P300-based brain-computer interface (BCI)? *Neuroscience Letters* **2009**, *462*, 94–98.
6. Lotte, F.; Faller, J.; Guger, C.; Renard, Y.; Pfurtscheller, G.; Lécuyer, A.; Leeb, R., Combining BCI with Virtual Reality: Towards New Applications and Improved BCI. In *Towards Practical Brain-Computer Interfaces: Bridging the Gap from Research to Real-World Applications*; Allison, B.Z.; Dunne, S.; Leeb, R.; Del R. Millán, J.; Nijholt, A., Eds.; Springer Berlin Heidelberg: Berlin, Heidelberg, 2013; pp. 197–220.
7. Jure, F.A.; Carrere, L.C.; Gentiletti, G.G.; Tabernig, C.B. BCI-FES system for neuro-rehabilitation of stroke patients. *Journal of Physics: Conference Series* **2016**, *705*, 012058.
8. Clerc, M.; Bougrain, L.; Lotte, F. *Brain-computer interfaces. 2, Technology and applications*; p. 331.
9. Riener, R.; Seward, L.J. Cybathlon 2016. *2014 IEEE International Conference on Systems, Man, and Cybernetics (SMC)* **2014**, pp. 2792–2794.
10. Huggins, J.E.; Alcaide-Aguirre, R.E.; Hill, K. Effects of text generation on P300 brain-computer interface performance. *Brain-Computer Interfaces* **2016**, *3*, 112–120.
11. Ramele, R.; Villar, A.J.; Santos, J.M. BCI classification based on signal plots and SIFT descriptors. 4th International Winter Conference on Brain-Computer Interface, BCI 2016; IEEE: Yongpyong, 2016; pp. 1–4.
12. Knuth, K.H.; Shah, A.S.; Truccolo, W.A.; Ding, M.; Bressler, S.L.; Schroeder, C.E. Differentially Variable Component Analysis: Identifying Multiple Evoked Components Using Trial-to-Trial Variability. *Journal of Neurophysiology* **2006**, *95*.
13. Alvarado-González, M.; Garduño, E.; Bribiesca, E.; Yáñez-Suárez, O.; Medina-Bañuelos, V.; Bribiesca, E. P300 Detection Based on EEG Shape Features. *Computational and Mathematical Methods in Medicine* **2016**, *2016*, 1–14.
14. Yamaguchi, T.; Fujio, M.; Inoue, K.; Pfurtscheller, G. Design Method of Morphological Structural Function for Pattern Recognition of EEG Signals During Motor Imagery and Cognition. 2009 Fourth International Conference on Innovative Computing, Information and Control (ICICIC). IEEE, 2009, pp. 1558–1561.
15. Hartman, a.L. *Atlas of EEG Patterns*; Vol. 65, 2005; pp. E6–E6.

16. Hu, L.; Mouraux, A.; Hu, Y.; Iannetti, G.D. A novel approach for enhancing the signal-to-noise ratio and detecting automatically event-related potentials (ERPs) in single trials. *NeuroImage* **2010**, *50*, 99–111.
17. Farwell, L.A.; Donchin, E. Talking off the top of your head: toward a mental prosthesis utilizing event-related brain potentials. *Electroencephalography and clinical neurophysiology* **1988**, *70*, 510–23.
18. Renard, Y.; Lotte, F.; Gibert, G.; Congedo, M.; Maby, E.; Delannoy, V.; Bertrand, O.; Lécuyer, A. OpenViBE: An Open-Source Software Platform to Design, Test, and Use Brain–Computer Interfaces in Real and Virtual Environments. *Presence: Teleoperators and Virtual Environments* **2010**, *19*, 35–53.
19. Liang, N.; Bougrain, L. Averaging techniques for single-trial analysis of oddball event-related potentials. *4th International Brain-Computer ...* **2008**, pp. 1–6.
20. Lowe, G. SIFT - The Scale Invariant Feature Transform. *International Journal* **2004**, *2*, 91–110.
21. Vedaldi, A.; Fulkerson, B. VLFeat - An open and portable library of computer vision algorithms. *Design* **2010**, *3*, 1–4.
22. Boiman, O.; Shechtman, E.; Irani, M. In defense of nearest-neighbor based image classification. *26th IEEE Conference on Computer Vision and Pattern Recognition, CVPR* **2008**.
23. Riccio, A.; Simione, L.; Schettini, F.; Pizzimenti, A.; Inghilleri, M.; Belardinelli, M.O.; Mattia, D.; Cincotti, F. Attention and P300-based BCI performance in people with amyotrophic lateral sclerosis. *Frontiers in Human Neuroscience* **2013**, *7*, 732.
24. Brunner, C.; Blankertz, B.; Cincotti, F.; Kübler, A.; Mattia, D.; Miralles, F.; Nijholt, A.; Otal, B. BNCI Horizon 2020 – Towards a Roadmap for Brain / Neural Computer Interaction. *Lecture Notes in Computer Science* **2014**, *8513*, 475–486.
25. Schalk, G.; McFarland, D.J.; Hinterberger, T.; Birbaumer, N.; Wolpaw, J.R. BCI2000: a general-purpose brain-computer interface (BCI) system. *IEEE transactions on bio-medical engineering* **2004**, *51*, 1034–43.
26. Tibon, R.; Levy, D.A. Striking a balance: analyzing unbalanced event-related potential data. *Frontiers in psychology* **2015**, *6*, 555.